

4. Veerasingam, S., Saha, M., Suneel, V., Vethamony, P., Rodrigues, A. C., Bhattacharyya, S. and Naik, B. G., Characteristics, seasonal distribution and surface degradation features of microplastic pellets along the Goa Coast, India. *Chemosphere*, 2016, **159**, 496–505.
5. Veerasingam, S., Mugilarasan, M., Venkatachalapathy, R. and Vethamony, P., Influence of 2015 flood on the distribution and occurrence of microplastic pellets along the Chennai coast, India. *Mar. Pollut. Bull.*, 2016, **109**, 196–204.
6. Vidyasakar, A. *et al.*, Macrodebris and microplastic distribution in the beaches of Rameswaram Coral Island, Gulf of Mannar, south-east coast of India: a first report. *Mar. Pollut. Bull.*, 2018, **137**, 610–616.
7. Khalik, W. M. A. W. M., Ibrahim, Y. S., Anuar, S. T., Govindasamy, S. and Baharuddin, N. F., Microplastics analysis in Malaysian marine waters: a field study of Kuala Nerus and Kuantan. *Mar. Pollut. Bull.*, 2018, **135**, 451–457.
8. Mintenig, S. M., Loder, M. G. J., Primpke, S. and Gerdt, G., Low numbers of microplastics detected in drinking water from groundwater sources. *Sci. Total Environ.*, 2019, **648**, 631–635.
9. Zbyszewski, M. and Corcoran, P. L., Distribution and degradation of fresh water plastic particles along the beaches of Lake Huron, Canada. *Water Air Soil Pollut.*, 2011, **220**, 365–372.
10. Zhao, S., Zhu, L. and Li, D., Microplastic in three urban estuaries, China. *Environ. Pollut.*, 2015, **206**, 597–604.
11. Schymanski, D., Goldbeck, C., Humpf, H. U. and Furst, P., Analysis of microplastics in water by micro-Raman spectroscopy: release of plastic particles from different packaging into mineral water. *Water Res.*, 2018, **129**, 154–162.
12. Asensio, R. C., Moya, M. S. A., Roja, J. M. D. L. and Gomez, M., Analytical characterization of polymers used in conservation and restoration by ATR-FTIR spectroscopy. *Anal. Bioanal. Chem.*, 2009, **395**, 2081–2096.
13. Jung, M. R. *et al.*, Validation of ATR FT-IR to identify polymers of plastic marine debris, including those ingested by marine organisms. *Mar. Pollut. Bull.*, 2018, **127**, 704–716.
14. Fries, E., Dekiff, J. H., Willmeyer, J., Nuelle, M. T., Ebert, M. and Remy, D., Identification of polymer types and additives in marine microplastic particles using pyrolysis-GC/MS and scanning electron microscopy. *Environ. Sci.: Process. Impacts*, 2013, **15**, 1949–1956.
15. Kang, H. J., Park, H. J., Kwon, O. K., Lee, W. S., Jeong, D. H., Ju, B. K. and Kwon, J. H., Occurrence of microplastics in municipal sewage treatment plants: a review. *Environ. Health Toxicol.*, 2018, **33**, 1–8.
16. Mugilarasan, M., Venkatachalapathy, R., Sharmila, N. and Gurumoorthi, K., Occurrence of microplastic resin pellets from Chennai and Tinnakkara Island: towards the establishment of background level for plastic pollution. *Indian J. Mar. Sci.*, 2017, **46**, 1210–1212.
17. Sathish, N., Jeyasanta, K. I. and Patterson, J., Abundance, characteristics and surface degradation features of microplastics in beach sediments of five coastal areas in Tamil Nadu, India. *Mar. Pollut. Bull.*, 2019, **142**, 112–118.
18. [www.arcgis.com](http://www.arcgis.com)
19. Browne, M. A., Crump, P., Niven, S. J., Teuten, E., Tonkin, A., Galloway, T. and Thompson, R., Accumulation of microplastic on shorelines worldwide: sources and sinks. *Environ. Sci. Technol.*, 2011, **45**, 9175–9179.

ACKNOWLEDGEMENT. This study was supported by the University Grants Commission, New Delhi.

Received 7 June 2019; revised accepted 6 August 2019

doi: 10.18520/cs/v117/i11/1879-1885

## Transcriptomic analysis of chilling-treated tobacco (*Nicotiana tabacum*) leaves reveals chilling-induced lignin biosynthetic pathways

PeiLu Zhou<sup>1,2</sup>, QiYao Li<sup>1</sup>, Guang Liang Liu<sup>1</sup>, Na Xu<sup>1</sup>, Yin Ju Yang<sup>1</sup>, Yi Wang<sup>1</sup>, Wen Long Zeng<sup>3</sup>, Shu Sheng Wang<sup>1</sup> and Ai Guo Chen<sup>1,\*</sup>

<sup>1</sup>Key Laboratory of Tobacco Biology and Processing, Ministry of Agriculture, Tobacco Research Institute of Chinese Academy of Agricultural Sciences, Qingdao 266101, People's Republic of China

<sup>2</sup>Tianjin Agricultural University, Tianjin 300384, People's Republic of China

<sup>3</sup>Longyan Tobacco Agricultural Science Institute, Longyan, Fujian 364000, People's Republic of China

**Chilling stress is one of the most important environmental stresses for chilling-sensitive species. The present study conducted RNA-Seq and WGCNA analysis to clarify the correlation patterns among genes of different treatments in tobacco (*Nicotiana tabacum*). A total of 10,355 DEGs were found in chilling treatment relative to control treatment. Additionally, functional annotations revealed that 48 genes were found to be specifically expressed in lignin biosynthesis pathway in tobacco seedlings under chilling stress. Our results revealed that the biosynthesis of caffeoyl-CoA was regulated by *HCT* and *C3H*. Furthermore, the G-type lignin biosynthesis branch was enhanced under low temperature, which contributed to an increase in lignin content and changes in lignin composition, indicating that G-type lignin may play an important role in tobacco's resistance to chilling stress.**

**Keywords:** Chilling stress, lignin biosynthesis, *Nicotiana tabacum*, transcriptomic, WGCNA.

CHILLING stress is one of the environmental factors that restrict plant growth and geographical distribution. Plants have evolved a number of sophisticated mechanisms to rapidly respond to changes in the environment and different types of defense mechanisms that protect plants from chilling stress. The synthesis of compounds in the phenylpropanoid pathway ([Supplementary Figure 1](#)) fulfills a wide range of such functions, including plant development and interactions with the environment<sup>1</sup>.

The phenylpropanoid metabolic pathway mainly starts with phenylalanine ([Supplementary Figure 1](#)) and provides the precursors of lignin, which is quantitatively the second most common biopolymer on Earth, following cellulose. The intermediates and products of the phenylpropanoid pathway regulate tobacco growth and

\*For correspondence. (e-mail: [chenaiguo@caas.cn](mailto:chenaiguo@caas.cn))

development<sup>2</sup>. Lignin is a major component of plant cell walls and provides mechanical strength to tree trunks and confers impermeability to vascular tissues<sup>3</sup>. It is mainly involved in defense mechanisms against biotic and abiotic stresses<sup>4</sup>.

About 10 key enzymes are involved in the biosynthesis of lignin in the phenylpropanoid metabolic branch ([Supplementary Figure 1](#)). Therefore, under chilling stress, the induced expression of these enzymes can also be utilized as tolerance indices in plants<sup>5,6</sup>. The phenylpropanoid metabolic pathway is activated by cold stress. Phenylalanine ammonia-lyase (PAL), hydroxycinnamoyl-CoA shikimate hydroxycinnamoyl transferase (HCT) and cinnamyl-alcohol dehydrogenase (CAD) are upregulated in the winter barley cultivar Luxor leaves after cold treatment<sup>7</sup>. Similarly, the expression of *C3H* (CYP98A3) in *Rhododendron* leaf tissues was upregulated upon exposure to the cold, suggesting its role in acclimation to low temperatures<sup>8</sup>. In barley leaves, lignin gene expression, including *CAD*, is upregulated under cold stress<sup>7</sup>.

Earlier researches have shown that changes in plant lignin content are influenced by stresses, and lignin synthesis plays an important role in complex genetic and physiological regulatory pathways<sup>9,10</sup>. However, investigations on the main pathway of lignin biosynthesis in tobacco in response to low temperature stress are limited. The aim of the present study was to elucidate the mechanism underlying the transcriptional regulation of lignin biosynthesis under chilling stress by assessing differentially expressed genes (DEGs) between plants subjected to chilling treatment and those exposed to normal temperatures using weighted gene co-expression network analysis (WGCNA).

Seven-leaf-old tobacco (*Nicotiana tabacum*, cv. K326) pot-grown plants were employed as experimental materials and propagated in growth chambers (DPGX-350B, Ningbo Prandt Instrument Co Ltd, China) at 25 ± 2°C, 14 h light/10 h dark photoperiod, and 65–75% relative humidity (RH). The second unfolded leaf forming the shoot apex was collected from each plant after 25°C or 4°C treatment for 12 h or 24 h respectively. The treatment was performed in triplicates, and the leaves of each treatment were pooled into one composite sample. After harvesting, the samples were immediately placed in liquid nitrogen and then stored at –80°C until analysis.

Total RNA was extracted and purified from untreated and chilling-treated tobacco leaves that were collected after 0 h, 12 h and 24 h using a TaKaRa MiniBEST plant RNA extraction kit (Takara Bio Inc., Dalian, China) based on the manufacturer's recommendations. RNA degradation and contamination were monitored on 1% agarose gels. RNA concentration was measured using a Qubit® RNA assay kit in a Qubit® 2.0 Fluorometer (Life Technologies, CA, USA). Samples that had an A260/A280 within the range of 1.9 to 2.1 and an A260/A230 > 2.0 were used in subsequent analyses. RNA

integrity was assessed using an RNA Nano 6000 assay kit on a Bioanalyzer 2100 system (Agilent Technologies, CA, USA).

Approximately 3 µg RNA per sample was used as input material for the RNA sample preparations. Sequencing libraries were generated using NEBNext® Ultra™ RNA Library Prep Kit for Illumina® (NEB, USA), following the manufacturer's recommendations, and index codes were added to attribute sequences to each sample.

The tobacco genome and gene model annotation files were downloaded from the Tobacco Genome Annotation Project (*Nicotiana tabacum* Ntab-TN90v, <https://www.ncbi.nlm.nih.gov/genome/425>). The index of the reference genome was built using Bowtie v2.2.3, and paired-end clean reads were aligned to the reference genome using TopHat v2.0.12. All the RNA-Seq raw data generated in this study were deposited in the sequence read archive (SRA) of National Centre for Biotechnology Information (NCBI) (accession number SRP129465).

HTSeq v0.6.1 was used to count the number of reads that were mapped to each gene. Fragments per kilobase per million reads (FPKM) values were used to normalize the expression levels of gene from RNA-Seq<sup>11</sup>. In subsequent analysis, FPKM value >1 was set as the threshold of gene transcriptional activity screening.

Differential expression analysis of untreated and chilling-treated tobacco leaves (three biological replicates per condition) was performed using the DESeq R package (1.18.0). Sequences were deemed to be significantly differentially expressed when the adjusted *P*-value was <0.05 and there was at least a two-fold change ( $|\log_2\text{fold-change}| \geq 1$ ) in FPKM values between the two libraries.

Databases like Kyoto Encyclopedia of Genes and Genomes (KEGG) database help us to understand the high-level functions and utilities of a biological system (<http://www.genome.jp/kegg/>). KOBAS software was used to test the statistical enrichment of DEGs in KEGG pathways.

The WGCNA R package (we looked up the relevant program code and R tutorial through the official website of WGCNA: <https://horvath.genetics.ucla.edu/html/CoexpressionNetwork/Rpackages/WGCNA/Tutorials/>) was used to analyse pairwise correlations between all genes across the measured samples (Langfelder and Horvath 2008). The weighted network uses a soft threshold for Pearson correlation between the expression profiles of any two samples. Average linkage hierarchical clustering was conducted to group transcripts based on topological overlap dissimilarity based on their network connection strengths. Modules were identified with a dynamic tree-cutting algorithm, with a minimum module size of two genes, and merged with the MEDissThres parameter for 0.05. Their interactive network was visualized using Cytoscape\_v3.4.0 with the edges file.

Selected DEGs in the tobacco samples subjected to chilling were validated using quantitative real time

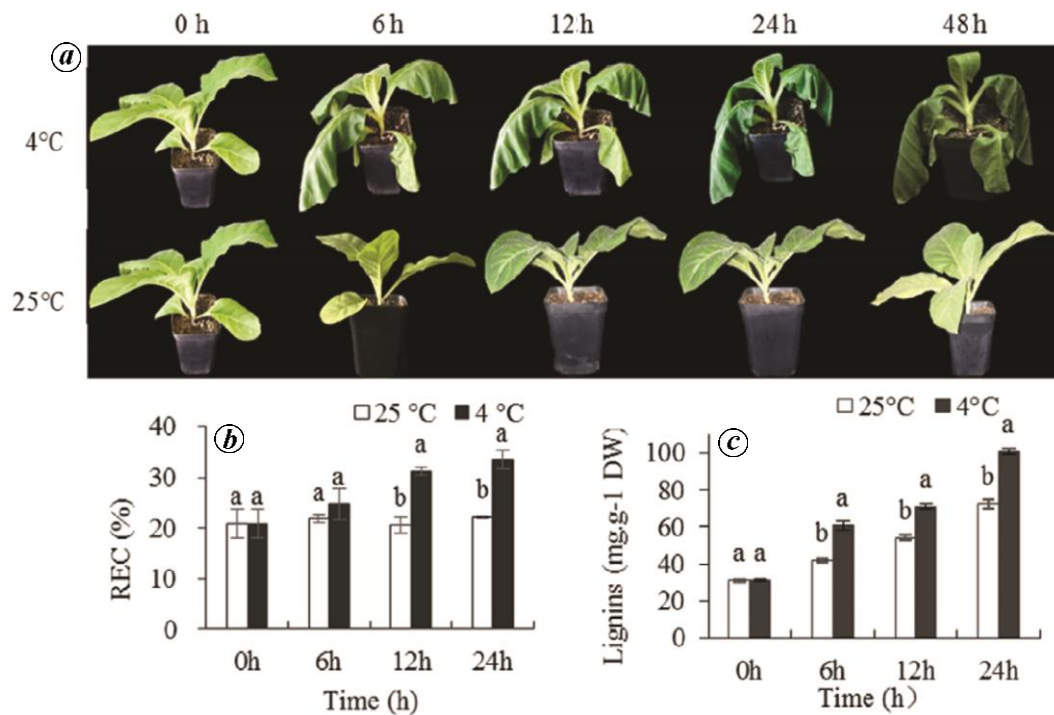


**Figure 1.** Phenotypes of tobacco seedlings subjected to chilling stress. *a*, Comparison of tobacco seedlings exposed to 4°C and 25°C temperatures for 0 h, 6 h, 12 h, 24 h and 48 h. *b*, Relative electrolytic conductivity (REC) of tobacco seedlings exposed to 4°C and 25°C temperatures. The values are the means of three replicates. Vertical bars indicate standard errors. *c*, Lignin content of tobacco seedlings exposed to 4°C and 25°C. Three biological replicates were used in each treatment. Values are presented as the mean  $\pm$  SE of three biological replicates. Lowercase letters (a and b) indicate significant differences in tobacco seedlings subjected to 4°C and 25°C temperatures.

polymerase chain reaction (qRT-PCR). Total RNA extraction and cDNA synthesis were performed as described earlier. Of the significant DEGs, 10 genes exhibiting similar expression patterns in both treatments were selected for validation analysis. The primers used for qRT-PCR were designed using Primer Premier 6.0 and are listed in [Supplementary Table 1](#). qRT-PCR was performed on an Applied Biosystems 7500 Real-Time PCR System using SYBR Premix Ex TaqII (Tli RNaseH Plus) (Takara Bio Inc., Dalian, China). Three biological replicates for each sample and three technical replicates for each biological sample were analysed. The constitutively expressed housekeeping gene *actin* from tobacco was used as reference. Changes in the relative gene expression levels were calculated using the  $2^{-\Delta\Delta Ct}$  method.

Lignin content was determined using a lignin content kit (Cominbio, Suzhou, China) according to the manufacturer's recommendations. To measure relative electrolytic conductivity (REC)<sup>12</sup>, 10 leaf discs (0.8 cm in diameter) were placed inside 20 ml of distilled water and vacuumed for 30 min, and then surged for 3 h to measure the initial electric conductance (S1) at 25°C. The mixture was then transferred to a cuvette and heated at 100°C for 30 min, later allowed to cool down to room temperature (25°C) and used in the determination of final electric conductance (S2). REC was calculated as follows:  $REC = S1 \times 100/S2$ .

To identify the effects of chilling stress on tobacco, seedlings subjected to 4°C (T) and 25°C (CK) treatment were compared. Seedlings grown in chilling conditions exhibited wilting, which increased in severity over time (Figure 1*a*). In addition, a significantly higher REC was observed after 12 h chilling treatment compared to the controls ( $P < 0.05$ , Figure 1*b*). Lignin content increased in seedlings subjected to chilling compared to those grown at 25°C (Figure 1*c*). Based on the observed phenotypes and changes in REC, samples collected at the 12 h and 24 h time period were used for RNA-Seq analysis.

To clarify the transcriptome changes of genes related to low temperature stress in tobacco, RNA-Seq was performed. A total of 666.9 million clean reads were generated from the 15 cDNA libraries, and 649.7 million high-quality ( $Q > 20$ ) 100 bp reads were selected for further analysis. Approximately 91.38–95.91% of the short clean reads were aligned against the *N. tabacum* reference genome. Around 88.74% to 95.35% of the reads could be uniquely mapped to the reference genome, and more than 30,000 genes were identified ([Supplementary Table 2](#)).

In the T 12 h versus CK 12 h seedlings, a total of 18,530 significant DEGs were identified, which consisted of 9725 upregulated and 8805 downregulated DEGs. Of the 17,287 significant DEGs in the T 24 h versus CK 24 h seedlings, 8959 were upregulated and 8328 were

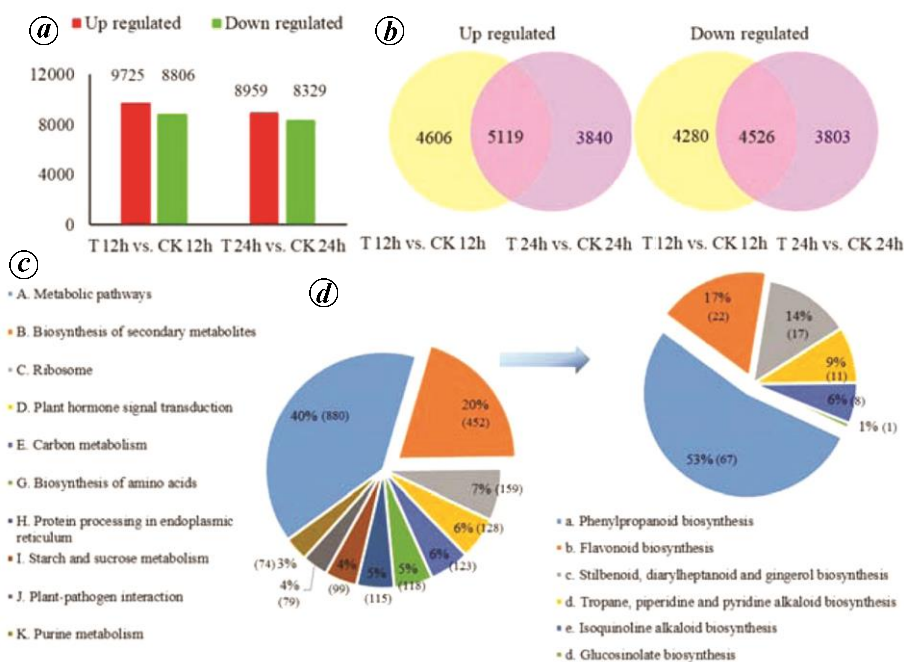


**Figure 2.** Overview of serial analysis of DEGs identified by pairwise comparisons of the four tobacco transcriptomes CK 12 h, CK 24 h, T 12 h, and T 24 h. *a*, Up- or downregulated DEGs in response to chilling stress in T 12 h versus CK 12 h and T 24 h versus CK 24 h. *b*, Venn diagram of up- and down-regulated DEGs after exposure to low temperature conditions. The separate and overlapping areas in the Venn diagrams represent the number of specifically expressed and co-expressed genes between different treatments. *c* and *d*, Functional annotation of DEGs related to the biosynthesis of secondary metabolites.

**Table 1.** Summary of genes involved in lignin biosynthesis

Gene name	EC number	Enzyme name	Number of DEGs
<i>PAL</i>	EC: 4.3.1.24	Phenylalanine ammonia-lyase	3
<i>CAH</i>	EC: 1.14.13.11	<i>Trans</i> -cinnamate 4-monooxygenase	3
<i>4CL</i>	EC: 6.2.1.12	4-Coumarate--CoA ligase	6
<i>C3H</i>	EC: 1.14.13.36	Coumaroylquininate (coumaroylshikimate) 3'-monooxygenase	2
<i>HCT</i>	EC: 2.3.1.133	Shikimate <i>O</i> -hydroxycinnamoyltransferase	5
<i>CCoAOMT</i>	EC: 2.1.1.104	Caffeoyl-CoA <i>O</i> -methyltransferase	7
<i>F5H</i>	EC: 1.14.-.-	Ferulate-5-hydroxylase	1
<i>CAD</i>	EC: 1.1.1.195	Cinnamyl-alcohol dehydrogenase	4
<i>POD</i>	EC: 1.11.1.7	Peroxidase	17
Total			48

downregulated (Figure 2 *a*). A total of 10,355 DEGs between the chilling-treated and control seedlings were identified after 12 h and 24 h of treatment, which included 5119 upregulated and 4526 downregulated DEGs (Figure 2 *b*).

Pathway-based enrichment analysis will help us further understand the biological function of DEGs. KEGG pathway analysis annotated 4642 DEGs to 121 different pathways, and the top 10 KEGG pathways are shown in Figure 2 *c*. Pathways showing the highest DEG enrichment were 'metabolic pathway' and 'biosynthesis of secondary metabolites' and 'ribosome'. In terms of metabolic function, biosynthesis of secondary metabolites

was further classified into six subcategories, which included phenylpropanoid biosynthesis, flavonoid biosynthesis, stilbenoid, diarylheptanoid and gingerol biosynthesis, tropane, piperidine and pyridine alkaloid biosynthesis, isoquinoline alkaloid biosynthesis and glucosinolate biosynthesis (Figure 2 *d*). These results indicated that various metabolic processes were active and a variety of metabolites were synthesized in the leaves of tobacco seedlings that were subjected to chilling stress. KEGG pathway analysis of the annotated tobacco transcriptome dataset assigned a total of 48 genes that encoded nine known enzymes to the lignin biosynthesis pathway (Table 1).

In order to better understand the gene expression network involved in lignin biosynthesis in tobacco, a gene co-expression network model was constructed by WGCNA package. Optional threshold parameter  $\beta$  ( $\beta = 10$ , [Supplementary Figure 2](#)) was identified and selected, and the WGCNA algorithm was utilized to transfer the correlation coefficient between genes into the adjacent coefficient, which was then used to calculate the dissimilarity of the topological overlap matrix. We finally obtained four gene modules ([Supplementary Figure 3 a](#)) based on hierarchical clustering of the calculated dissimilarity.

To identify modules that were significantly associated with lignin content and REC, WGCNA constructed a gene expression matrix and further validated the modules ([Supplementary Figure 3 b](#)), which were then illustrated in Cytoscape\_3.5.1 to depict their relationships ([Supplementary Figure 3 c](#)). We found that the MEturquoise and MEBrown modules were highly related to the lignin contents and REC. Thus, we focused on the MEturquoise and MEBrown modules, and the 18 genes (degree > 25) that showed greater connectivity were selected as hub genes for further analysis.

The expression of 18 genes in MEturquoise and MEBrown modules that were highly correlated with lignin biosynthesis, were considered as potential candidate genes involved in lignin biosynthesis. The expression patterns of these 18 genes under chilling treatment were calculated ([Supplementary Figure 4](#)). We found that the genes encoding the same enzyme had different expression levels. For example, *gene\_15825* and *gene\_57109* encoded a PAL enzyme, but *gene\_15825* had higher expression levels under chilling treatment compared to the control. Three genes, *gene\_62870*, *gene\_67175* and *gene\_72324*, encoded a C4H enzyme, but only *gene\_62870* and *gene\_67175* showed higher expression. All candidate genes that exhibited high connectivity were selected, as suggested by the results of WGCNA ([Supplementary Figure 3 d](#)) *gene\_76120* (*CCoAOMT*) and *gene\_52281* (*POD*) were excluded because of their low connectivity. Hence, based on our analysis of expression patterns of these 18 hub genes, we identified eight candidate genes that enhanced lignin biosynthesis in tobacco under chilling stress. These candidate genes included *gene\_15825* (*PAL*), *gene\_62870* (*C4H*), *gene\_67175* (*C4H*), *gene\_85448* (*4CL*), *gene\_34078* (*HCT*), *gene\_34916* (*C3H*), *gene\_1089* (*CCoAOMT*) and *gene\_66975* (*CAD*). Further functional analysis of these candidate genes might be useful to define the main pathway of lignin synthesis under low temperature conditions.

Additionally we verified the transcriptional regulation revealed by RNA-Seq through biologically independent experiment using qRT-PCR. A total of 18 genes, including the eight candidate genes and 10 genes randomly selected from DEGs with large differences in expression were chosen and used in the design of gene-specific

primers ([Supplementary Table 1](#)). The qRT-PCR results showed that the eight candidate genes were upregulated under chilling stress and coincided with the RNA-Seq data (Figure 3). Moreover, for all the randomly selected genes, we found significant expression differences at low temperatures. Although there were differences in gene expression multiples between RNA-Seq and qRT-PCR data, all the validated genes exhibited similar expression patterns that agreed with the results of RNA-Seq ([Supplementary Figure 5](#)).

Chilling stress is one of the most critical abiotic stresses for chilling-sensitive species. It is a serious threat to the sustainability of crop production and quality. However, plants have adopted a complex system to perceive and respond to chilling stress over the course of evolution. Lignin is a cell wall component that also serves as an antioxidant, which protects cells against chilling-induced oxidative damage<sup>3,13</sup>. The type of cell wall (primary and secondary), tissues and organs<sup>14</sup>, lignin biosynthesis, and deposition in the cell walls in plants are affected by various environmental conditions, such as drought, low temperature, UV-B radiation, and even the pathogen attacks<sup>10</sup>. The lignin content of *ex vitro* poplar seedlings increased when they were grown at 10°C, whereas no significant changes in *in vitro* seedlings were observed<sup>15</sup>. Lignin content may be positively correlated with the annual average temperature in latewood *Picea abies*<sup>16</sup>. Increased rates of lignin units under cold can be used as a shielding mechanism of plants due to changes in cell wall composition<sup>17</sup>. In our findings, we observed an elevated level of lignin content in tobacco leaves exposed to low temperature conditions, suggesting that lignification could be an important plant mechanism for resisting environmental stress.

In plants, lignin biosynthesis is the result of a complex gene regulatory network<sup>18</sup>, where several enzymes are involved and may respond differently to biotic and abiotic stresses ([Supplementary Figure 1](#)). To elucidate the main route of lignin biosynthesis induced by chilling stress in tobacco plant varieties, we used RNA-Seq to conduct a transcriptome analysis of tobacco following chilling treatment and WGCNA analysis to describe correlation patterns among genes across transcriptome samples. Notably, the MEturquoise and MEBrown modules were specifically and highly related to lignin content ([Supplementary Figure 3 b](#)), and all of the hub genes in MEBrown module exhibited significant upregulation in the chilling treatment samples ([Supplementary Figure 3 d](#) and [Supplementary Figure 3](#)). Contents of lignin and soluble phenols were closely related in the leaves of *Triticum aestivum* plants exposed to 2°C temperature<sup>19</sup>. Lignin accumulated in tillering nodes where the increase in the amount of soluble phenolic compounds correlated with the elevated PAL activity<sup>20</sup>. PAL is the first enzyme of the phenylpropanoid pathway that catalyses the deamination of phenylalanine into *trans*-cinnamic acid<sup>21</sup>.

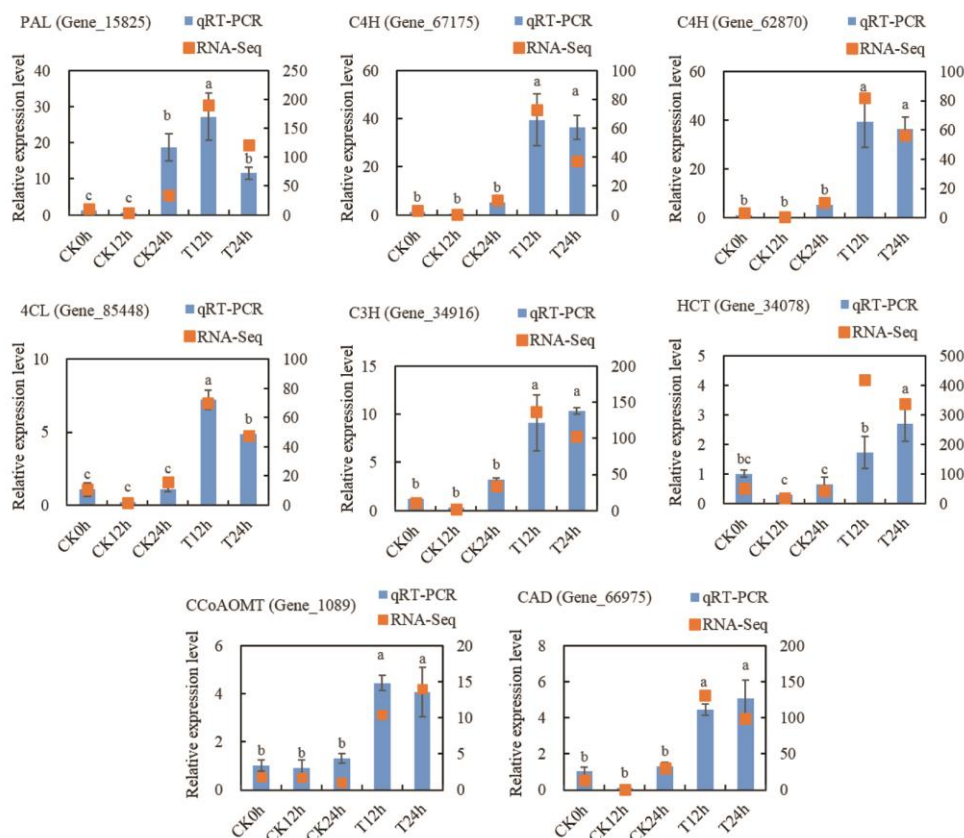


**Figure 3.** Expression profiles of validation genes in control- and chilling-treatment of tobacco leaves by qRT-PCR analysis. Relative levels of gene expression were calculated using the *actin* gene. The x-axis indicates the five samples. The y-axis shows the expression levels: the left represents qRT-PCR; the right represents FPKM. All PCR reactions were performed three times. The values are presented as the mean  $\pm$  SD of three independent extractions. Lowercase letters (a, b and c) indicate the significant differences of tobacco seedling between 4°C and 25°C treatment.

Decreased PAL activity can result in an increase in free L-phenylalanine<sup>20</sup>. The three enzymes of the phenylpropanoid pathway, PAL, C4H, and 4CL, are highly conserved among plant species as they are important for normal growth and development. The cold-induced upregulation of *PAL*, *C4H* and *4CL* results in an increased flow of metabolic substances into the phenylpropanoid pathway. Enzyme *C3H* (a cytochrome P450-dependent monooxygenase) is involved in the biosynthesis of phenylpropanoids and lignin. The expression level of gene coding for *C3H* increased during acclimation of *Rhododendron* to cold<sup>22</sup>. A previous study has shown that coumaroyl quinate acid (*CGA*) is an important intermediate for lignin biosynthesis; thus, *CGA* levels are the result of a dynamic balance between the influx via the catalysis of *C3H* and *HQT* enzymes and outflux through the catalysis of *HCT* enzymes, which convert to caffeoyl-CoA<sup>23</sup>. However, caffeoyl shikimate acid is another intermediate in caffeoyl-CoA biosynthesis through the continuous catalysis by *HCT* and *C3H*. Here, the upregulation of *HCT* and *C3H* contributes to lignin biosynthesis through caffeoyl shikimate acid shunt rather than the coumaroyl quinate acid branch, as indicated by a lack of significant change in *HQT* expression in tobacco under chilling stress.

Lignin is composed of three basic units (H/G/S), and its biosynthesis belongs to different directions of phenylpropanoid pathway<sup>24</sup>. Similar to lignin content, growth in different environments, such as low temperature, apparently changes lignin composition due to the changes in the expression of several lignin biosynthesis genes at low temperature<sup>25</sup>. Caffeoyl-coenzyme A 3-O-methyltransferase (*CCoAOMT*) is a key enzyme involved in methylation reaction in lignin biosynthesis. The downregulation of *CCoAOMT* in *Pinus radiata*, *Medicago sativa*, and *Populus tremula*  $\times$  *Populus alba* plants leads to decreased lignin content and significant changes in G-type lignin rather than S-type lignin, indicating that *CCoAOMT* is mainly required for the biosynthesis of G-type lignin<sup>26–29</sup>. Bonawitz and Chapple<sup>30</sup> reported that lignin containing high proportion of G subunits undergoes a higher degree of crosslinking than lignin rich in S subunits, possibly rendering rigidity and hydrophobicity. Similar to the above study, *COMT* and *F5H* were proved to be important enzymes involved in lignin biosynthesis, participated in the synthesis of S-unit, and were possible regulatory targets to reduce S-type lignin contents in sugarcane by cold treatment<sup>31</sup>. In this study, *CAD* genes were also upregulated after cold treatment, which in turn

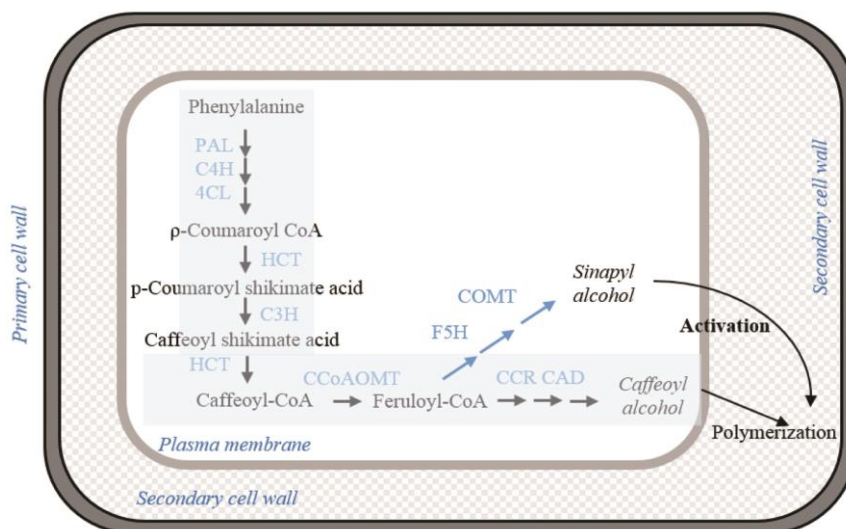


**Figure 4.** Proposed flux model of biochemical pathways leading to lignin biosynthesis in tobacco under chilling stress. The black and blue lines indicate enhanced synthetic pathways and weak change routes respectively. Enzyme names are listed in [Supplementary Figure 1](#).

promoted the synthesis of lignin<sup>7</sup>. In summary, this process might enhance the hardness and water retention of cell walls by increasing lignin content and changing lignin composition, thereby increasing resistance to chilling stress.

We have proposed a simplified model of lignin biosynthesis in tobacco leaves under chilling stress (Figure 4). However, this model is still in its initial stage and needs further improvement and optimization by scientific experiments. This model is a simplified version that responds to metabolic levels through transcriptional levels and does not involve post-translational regulation. Furthermore, this study still lacks information about how plants can sense low temperature signals to regulate the synthesis of lignin and its intermediates. Hence, to further improve this model, a systems biology approach is warranted.

Recent studies on lignin biosynthesis in tobacco have revealed that the biosynthesis of lignin precursor caffeoyl-CoA, primarily through the synthesis and degradation of caffeoyl shikimate acid by the catalysis of HCT and C3H enzymes rather than the branch involved in the synthesis and degradation of CGA, is catalysed by HQT, C3H and HCT enzymes. Furthermore, the G-type lignin biosynthesis branch of the lignin biosynthesis pathway in tobacco leaves was strengthened under low temperature, thereby increasing lignin content and altering lignin composition.

1. Croteau, R., Kutchan, T. M. and Lewis, N. G., Natural products (secondary metabolites). In *Biochemistry and Molecular Biology of Plants* (eds Buchanan, B., Gruissem, W. and Jones, R. L.), American Society of Plant Physiologists, Rockville, MD, USA, 2000, pp. 1250–1318.
2. Merali, Z., Mayer, M. J., Parker, M. L., Michael, A. J., Smith, A. C. and Waldron, K. W., Expression of a bacterial, phenylpropanoid-metabolizing enzyme in tobacco reveals essential roles

- of phenolic precursors in normal leaf development and growth. *Physiol. Plantarum.*, 2012, **145**(2), 260–274.
3. Humphreys, J. M. and Chapple, C., Rewriting the lignin roadmap. *Curr. Opin. Plant Biol.*, 2002, **5**, 224–229.
4. Vanholme, R., Morreel, K., Ralph, J. and Boerjan, W., Lignin engineering. *Curr. Opin. Plant Biol.*, 2008, **11**(3), 278–285.
5. Ali, M. B. and McNear Jr, D. H., Induced transcriptional profiling of phenylpropanoid pathway genes increased flavonoid and lignin content in Arabidopsis leaves in response to microbial products. *BMC Plant Biol.*, 2014, **14**, 84.
6. Wen, P. F., Chen, J. Y., Wan, S. B., Kong, W. F., Zhang, P. and Wang, W., Salicylic acid activates phenylalanine ammonia-lyase in grape berry in response to high temperature stress. *J. Plant Growth Regul.*, 2008, **55**, 1–10.
7. Janska, A., Aprile, A., Zamecnik, J., Cattivelli, L. and Ovesna, J., Transcriptional responses of winter barley to cold indicate nucleosome remodelling as a specific feature of crown tissues. *Funct. Integr. Genomic.*, 2011, **11**, 307–325.
8. Wei, H., Dhanaraj, A. L., Arora, R., Rowland, L. J., Fu, Y. and Sun, L., Identification of cold acclimation-responsive *Rhododendron* genes for lipid metabolism, membrane transport and lignin biosynthesis: Importance of moderately abundant ESTs in genomic studies. *Plant Cell Environ.*, 2006, **29**, 558–570.
9. Khaledian, Y., Maali-Amiri, R. and Talei, A., Phenylpropanoid and antioxidant changes in chickpea plants during cold stress. *Russ. J. Plant Physiol.*, 2015, **62**(6), 772–778.
10. Moura, J. C. M. S., Bonine, C. A. V., De Oliveira Fernandes Viana, J., Dormelas, M. C. and Mazzafera, P., Abiotic and biotic stresses and changes in the lignin content and composition in plants. *J. Integr. Plant Biol.*, 2010, **52**, 360–376.
11. Trapnell, C. *et al.*, Transcript assembly and quantification by RNA-seq reveals unannotated transcripts and isoform switching during cell differentiation. *Nat. Biotechnol.*, 2010, **28**(5), 511–515.
12. Cao, W. H., Liu, J., He, X. J., Mu, R. L., Zhou, H. L., Chen, S. Y. and Zhang, J. S., Modulation of ethylene responses affects plant salt-stress responses. *Plant Physiol.*, 2007, **143**, 707–719.
13. Miedes, E., Vanholme, R., Boerjan, W. and Molina, A., The role of the secondary cell wall in plant resistance to pathogens. *Front. Plant Sci.*, 2014, **5**, 358.
14. Grabber, J. H., Ralph, J., Lapierre, C. and Barriere, Y., Genetic and molecular basis of grass cell-wall degradability, I. Lignin-cell wall matrix interactions. *CR Biol.*, 2004, **327**, 455–465.

15. Hausman, J. F., Evers, D., Thiellement, H. and Jouve, L., Compared responses of poplar cuttings and *in vitro* raised shoots to short-term chilling treatments. *Plant Cell Rep.*, 2000, **19**, 954–960.
16. Gindl, W., Grabner, M. and Wimmer, R., The influence of temperature on latewood lignin content in treeline Norway spruce compared with maximum density and ring width. *Trees-Struct. Funct.*, 2000, **14**, 409–414.
17. Weng, J. K. and Chapple, C., The origin and evolution of lignin biosynthesis. *New Phytol.*, 2010, **187**, 273–285.
18. Rogers, L. A. and Campbell, M. M., The genetic control of lignin deposition during plant growth and development. *New Phytol.*, 2004, **164**, 17–30.
19. Olenichenko, N. and Zagoskina, N., Response of winter wheat to cold: production of phenolic compounds and l-phenylalanine ammonia lyase activity. *Appl. Biochem. Microbiol.*, 2005, **41**, 600–603.
20. Janas, K. M., Cvikrova, M., Palagiewicz, A. and Eder, J., Alterations in phenylpropanoid content in soybean roots during low temperature acclimation. *Plant Physiol. Biochem.*, 2000, **38**, 587–593.
21. El Kayal, W., Keller, G., Debayles, C., Kumar, R., Weier, D., Teulieres, C. and Marque, C., Regulation of tocopherol biosynthesis through transcriptional control of tocopherol cyclase during cold hardening in *Eucalyptus gunnii*. *Physiol. Plantarum.*, 2006, **126**, 212–223.
22. MacDonald, M. J. and D’Cunha, G. B., A modern view of phenylalanine ammonia lyase. *Biochem. Cell Biol.*, 2007, **85**, 273–282.
23. Valiñas, M. A., Lanteri, M. L., ten Have, A. and Balbina Andreu, A., Chlorogenic acid biosynthesis appears linked with suberin production in potato tuber (*Solanum tuberosum*). *J. Agric. Food Chem.*, 2015, **63**(19), 4902–4913.
24. Hisano, H., Nandakumar, R. and Wang, Z. Y., Genetic modification of lignin biosynthesis for improved biofuel production. *In vitro Cell. Dev. Biol. (Plant)*, 2009, **45**, 306–313.
25. Hu, R. *et al.*, Comparative transcriptome analysis revealed the genotype specific cold response mechanism in tobacco. *Biochem. Biophys. Res. Commun.*, 2016, **469**(3), 535–541.
26. Wagner, A. *et al.*, CCoAOMT suppression modifies lignin composition in *Pinus radiata*. *Plant J.*, 2011, **67**, 119–129.
27. Guo, D., Chen, F., Inoue, K., Blount, J. W. and Dixon, R. A., Downregulation of caffeic acid 3-*O*-methyltransferase and caffeoyl CoA 3-*O*-methyltransferase in transgenic alfalfa: impacts on lignin structure and implications for the biosynthesis of G and S lignin. *Plant Cell Online*, 2001, **13**, 73–88.
28. Guo, D., Chen, F., Wheeler, J., Winder, J., Selman, S., Peterson, M. and Dixon, R. A., Improvement of in-rumen digestibility of alfalfa forage by genetic manipulation of lignin *O*-methyltransferases. *Transgenic Res.*, 2001, **10**, 457–464.
29. Zhong, R., Morrison, W. H., Himmelsbach, D. S., Poole, F. L. and Ye, Z. H., Essential role of caffeoyl coenzyme A *O*-methyltransferase in lignin biosynthesis in woody poplar plants. *Plant Physiol.*, 2000, **124**, 563–578.
30. Bonawitz, N. D. and Chapple, C., The genetics of lignin biosynthesis: connecting genotype to phenotype. *Ann. Rev. Genet.*, 2010, **44**(1), 337–363.
31. dos Santos, A. B. *et al.*, Lignin biosynthesis in sugarcane is affected by low temperature. *Environ. Exp. Bot.*, 2015, **120**, 31–42.

**ACKNOWLEDGEMENTS.** This study was supported by the Fundamental Research Funds for Central Non-Profit Scientific Institution (1610232016019), Longyan Corporation of Fujian Tobacco Corporation (LYK201302), and the Agricultural Science and Technology Innovation Program (ASTIP-TRIC03).

Received 2 August 2018; revised accepted 5 August 2019

doi: 10.18520/cs/v117/i11/1885-1892

## The Sandan slot canyon in the Deccan Traps: its morphology and mode of origin

Pramodkumar S. Hire<sup>1,\*</sup>, Archana D. Patil<sup>2</sup> and Vishwas S. Kale<sup>3</sup>

<sup>1</sup>Department of Geography, HPT Arts and RYK Science College, Nashik 422 005, India

<sup>2</sup>Department of Geography, RNC Arts, JDB Commerce and NSC Science College, Nashik 422 101, India

<sup>3</sup>A6 Manmohan Society, Karvenagar, Pune 411 052, India

**Slot canyons, with extremely small width–depth ratios, are rare geomorphic features that develop under limited range of fluvial conditions. We report the occurrence of such an uncommon canyon, developed on the crest of the Western Ghats in the Deccan Traps. The canyon is a tourist hotspot. Geomorphic studies reveal that the Sandan slot canyon is 2–30 m wide and up to 100 m deep. Based on compelling field evidence we hypothesize that the morphology of the slot canyon is the product of the interplay between flash flood-induced excavation of a dyke and slope failures.**

**Keywords.** Dyke, flash flood, slot canyon, slope failure.

GORGES are one of the most common erosional sculpted forms in actively incising fluvial landscapes around the world. In comparison, extremely narrow, deep and slot-like bedrock gorges, commonly called slot canyons<sup>1</sup>, are rare and develop under limited range of fluvial conditions. Slot canyons have very small width–depth ratios (depth  $\geq$  width) and the canyon walls make up a larger proportion of the channel boundary or perimeter than the canyon bottom (base)<sup>1</sup>. Majority of the slot canyons documented in the geomorphic literature occur in southwest USA<sup>2</sup>, China<sup>3</sup> and Austria<sup>4</sup> in a variety of rocks (sandstone, conglomerate, granite, gneiss, basalt, etc.). Till date, slot canyons have not been documented in the Indian subcontinent.

Here we report the occurrence and geomorphic characteristics of such an uncommon slot canyon from the Deccan Traps. The roughly north-south-oriented Sandan slot canyon (SSC) developed in compound lava flows is situated near Samrad village (19°30′46″N and 73°41′11″E) (Figure 1 a) in Ahmednagar district, Maharashtra, India<sup>5</sup> and occurs on the crest of the Western Ghats Escarpment (Figure 1 b). The canyon is a popular tourist hot spot and is famous for exhilarating adventure sports such as giant swing, rappelling and flying fox.

The main objectives of this study are: (a) to document the downstream variations in the canyon morphology, and

\*For correspondence. (e-mail: pramodkumarhire@gmail.com)